The Chemistry of Oxygen in Galactic Diffuse Clouds

Helmut Wiesemeyer, Max-Planck-Institute for Radio Astronomy
Ringberg Workshop on Spectroscopy with SOFIA, 17 March 2015

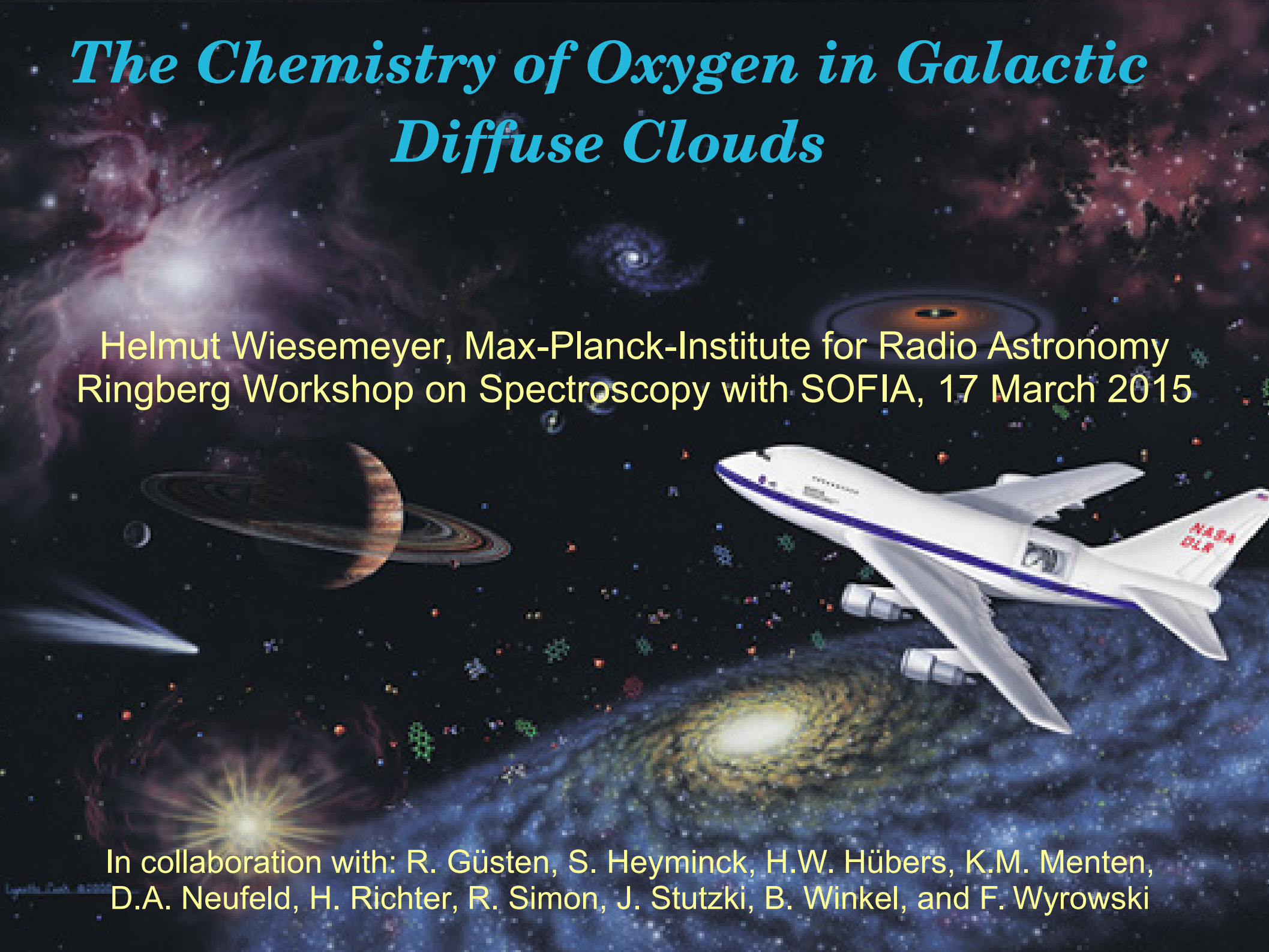

In collaboration with: R. Güsten, S. Heyminck, H.W. Hübers, K.M. Menten, D.A. Neufeld, H. Richter, R. Simon, J. Stutzki, B. Winkel, and F. Wyrowski

Survival of molecules in a harsh environment: dense knots exposed to strong UV radiation

HST image of Helix nebula
(Meixner et al. 2005, ApJ 130, 1784)

Types of Interstellar Clouds

A_V (min.)	Diffuse Atomic	Diffuse Molecular	Translucent	Dense Molecular
Defining Characteristic	$f^n_{H2} < 0.1$	$f^n_{H2} > 0.1$ $f^n_{C+} > 0.5$	$f^n_{C+} < 0.5$ $f^n_{CO} < 0.9$	$f^n_{CO} > 0.9$
A_V (min.)	0	~0.2	~1-2	~5-10
Typical n_H [cm-3]	10-100	100-500	500-5000 ?	> 104
Typical T [K]	30-100	30-100	15-50 ?	10-50
Observational Techniques	UV/Vis HI 21cm	UV/Vis IR abs mm abs	Vis (UV?) IR abs/em	IR abs mm em

Snow & Mc Call, 2006, ARA&A 44, 367

Chemistry of diffuse clouds

Three pillars:

- cold ion-neutral chemistry
- warm chemistry (endothermic reactions),
- grain surface reactions

& contribution from evolved stars

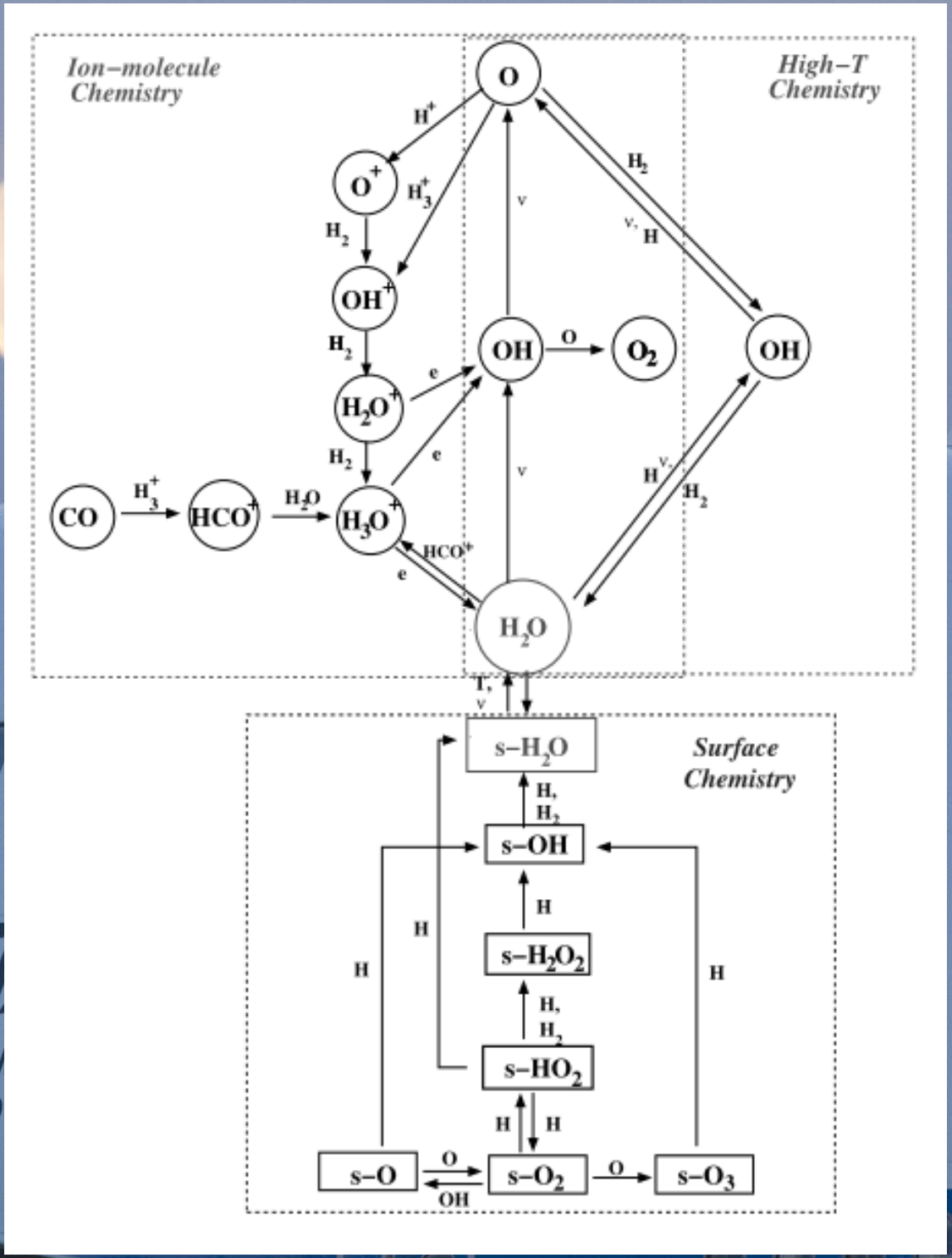

van Dishoeck et al. 2011, PASP 123, 138

The samples from the first and fourth quadrant (PRISMAS, ATLASGAL)

Table 2. Continuum sources and observed species.

	α (J2000)	δ (J2000)	l	b	v_{lsr}[km s^{-1}]		Species
G10.47	18:08:38.20	−19:51:50.0	10°472	0°027	(+48, +69)	(+58, +77)	CH, OH, OH^+
G10.62 (W31C)	18:10:28.69	−19:55:50.0	10.621	−0.387	(−3, +1)	(−10, +7)	CH, HF, O I, OH, OH^+
G34.26	18:53:18.70	01:14:58.0	34.257	0.154	(+55, +62)	(+58, +62)	HF, O I, OH, OH^+
W49N	19:10:13.20	09:06:12.0	43.166	0.012	(+2, +21)	(−1, +19)	CH, HF, O I, OH, OH^+
W51e2	19:23:43.90	14:30:30.5	49.489	−0.388	(+47, +72)	(+50, +61)	CH, HF, OH, OH^+
G327.29	15:53:08.55	−54:37:05.1	327.294	−0.580	(−72, −40)	(−49, −37)	CH, OH, OH^+
G330.95	16:09:53.01	−51:54:55.0	330.954	−0.182	(−102, −80)	(−91, −87)	CH, OH, OH^+
G332.83	16:20:10.65	−50:53:17.6	332.824	−0.548	(−55, −53)	(−59, −45)	OH, OH^+
G351.58	17:25:25.03	−36:12:45.3	351.581	−0.353	(−101, −89)	(−100, −87)	OH, OH^+

Notes. Columns 6 and 7 list the velocity ranges with OH and CH_3OH maser emission, respectively. For the fourth quadrant, OH and CH_3OH maser velocities are from Caswell 1998 and Caswell et al. 1995, for G34.26, from Fish et al. (2005) and Caswell et al. (1995), for W49N, from Deshpande et al. (2013) and Bartkiewicz et al. (2014), and for W51e2 from Fish et al. (2005) and Surcis et al. (2012), respectively.

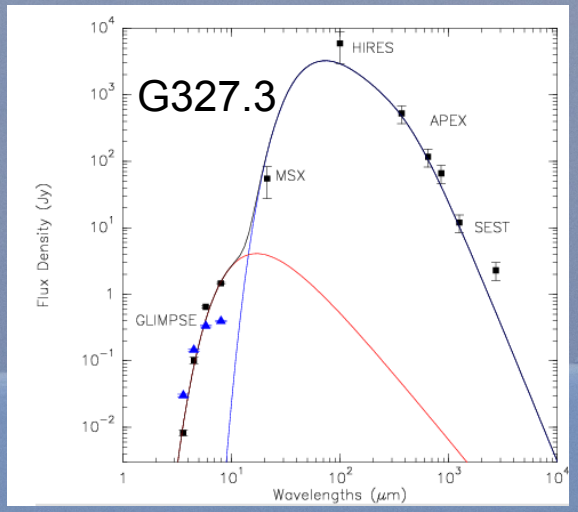

Wyrowski et al., 2006, A&A 454, L91 ↑

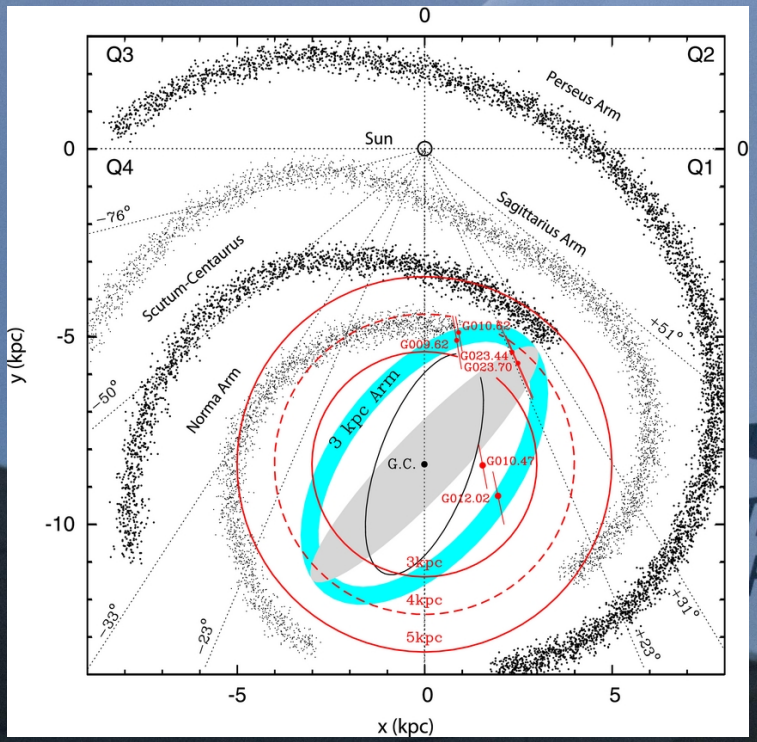

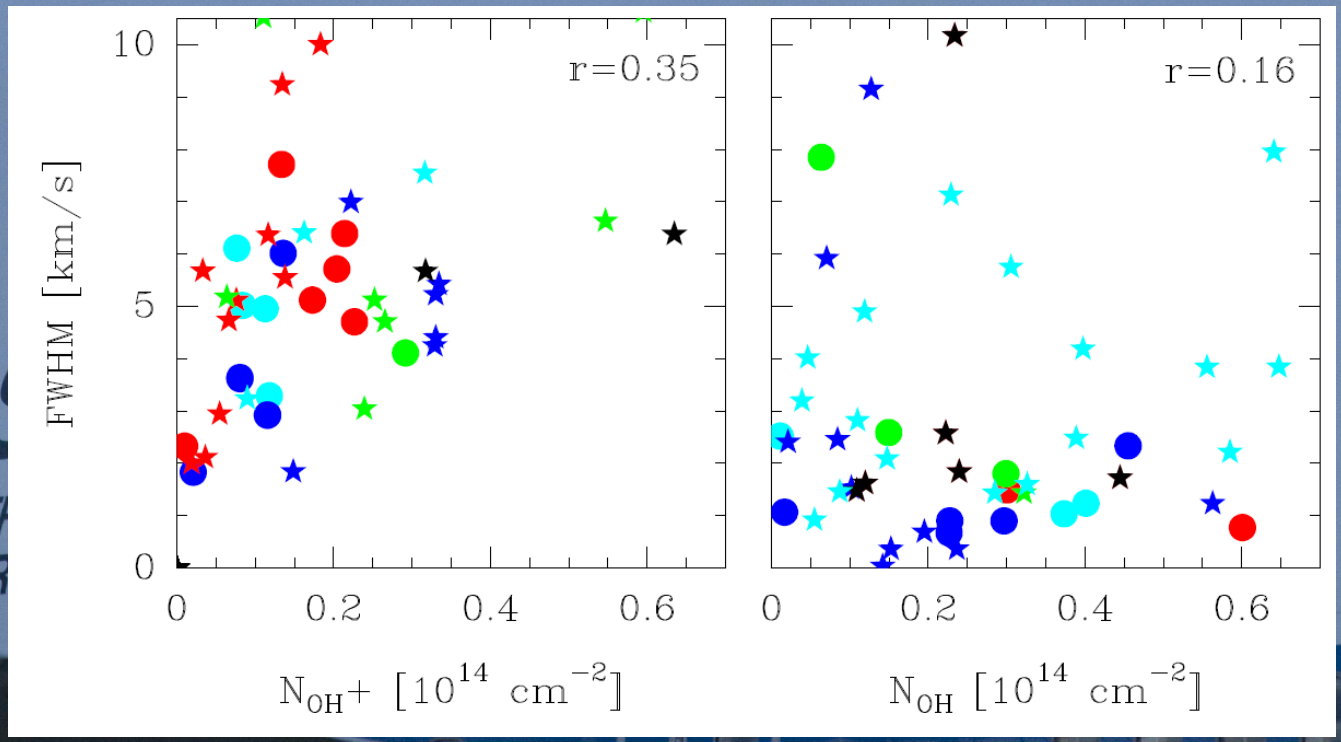

↑ Sanna et al., 2014, ApJ 781, 108

OH radio observations in diffuse clouds

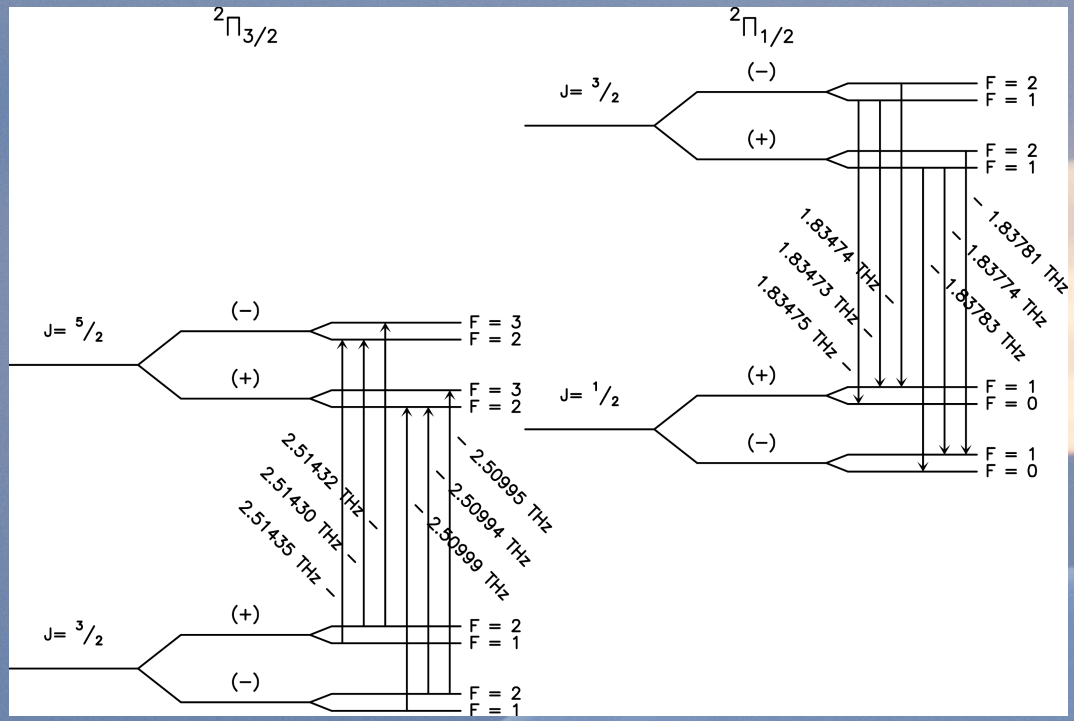

Table 3. Conditions in diffuse cloud models and coefficients for departure from LTE of the population in OH $^2\Pi_{3/2}$, $J = 3/2$ levels.

	Model 1	Model 2
	diffuse molecular	translucent
A_V	0.2	1
n_H [cm^{-3}]	100	1000
$f^n_{H_2}$	0.1	0.5
T_{gas} [K]	100	15
T_{dust}[K]	16	12
	departure coefficients	
$F = 1-$	1.7580	0.9966
$F = 2-$	1.7565	0.9963
$F = 1+$	1.7398	0.9991
$F = 2+$	1.7384	0.9987

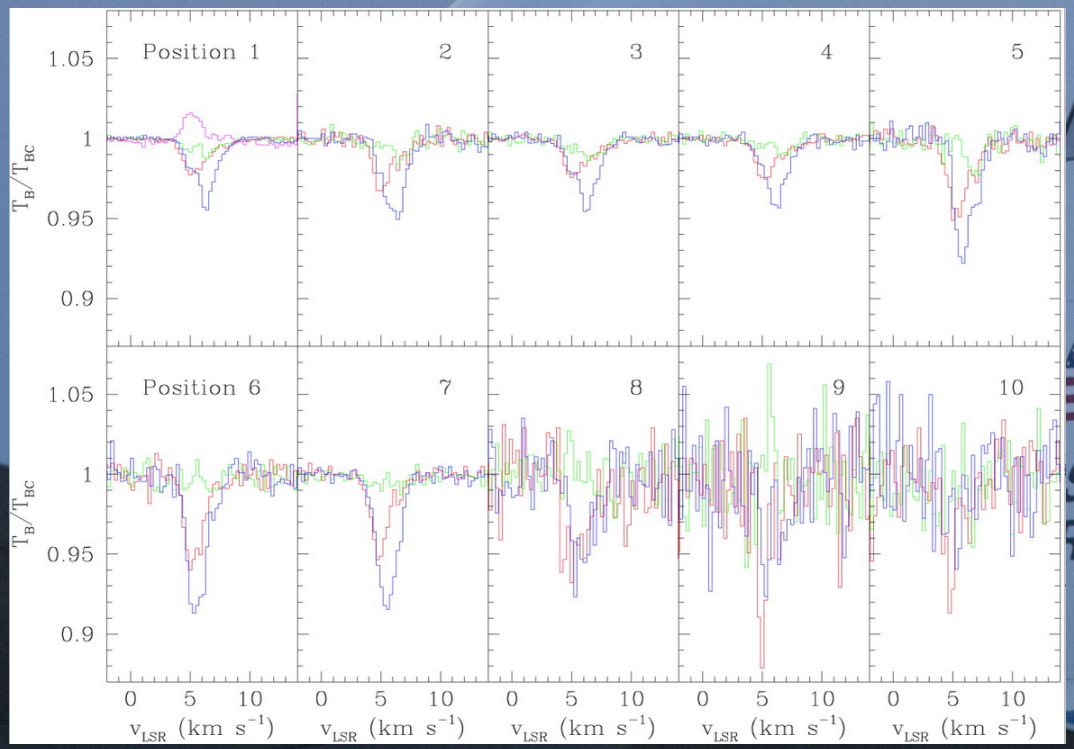

Neufeld et al. (2002):
NLTE effects in OH HFS lines
(W51, Arecibo data)

Equivalent width ratios	observed	LTE
1612 MHz	2	1
1665 MHz	1	5
1667 MHz	3	9
1720 MHz	-1	1

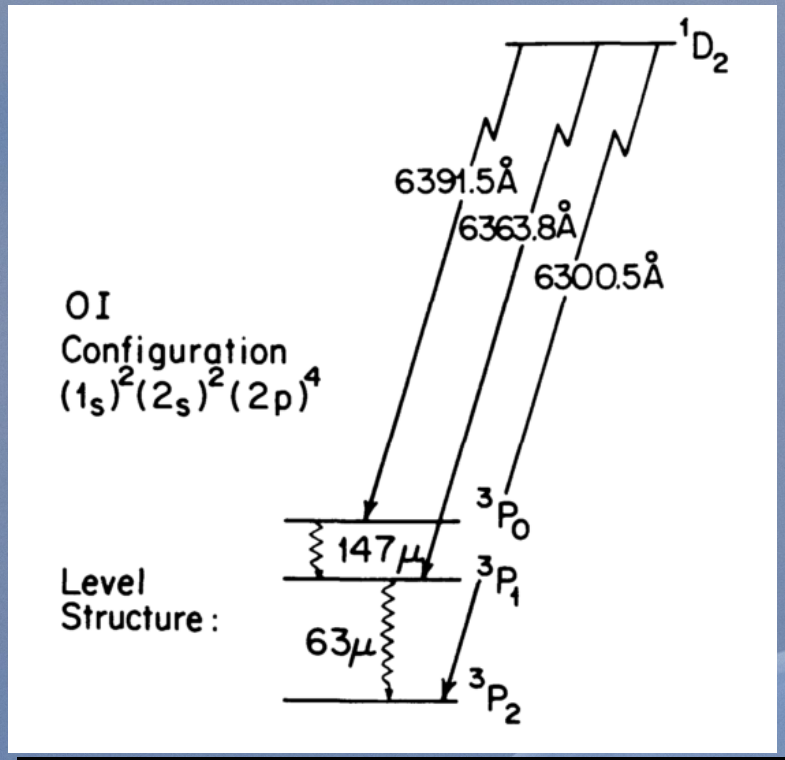

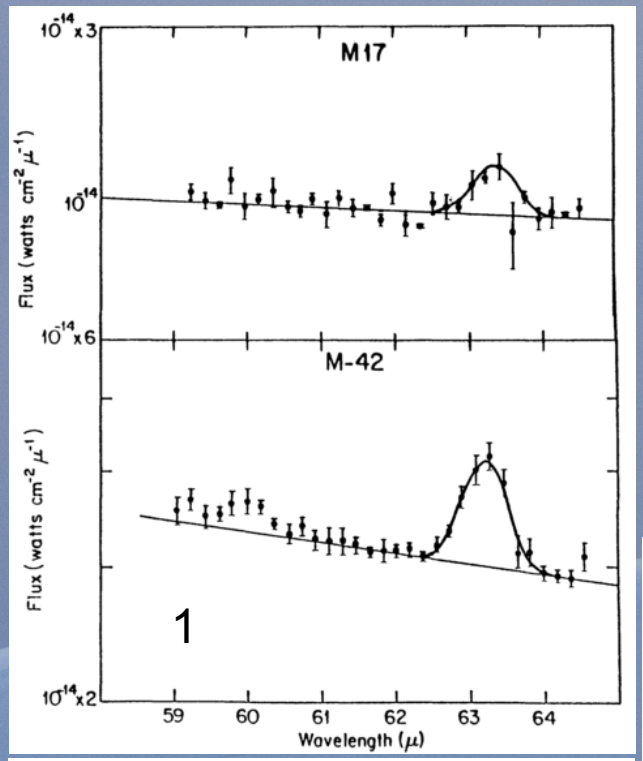

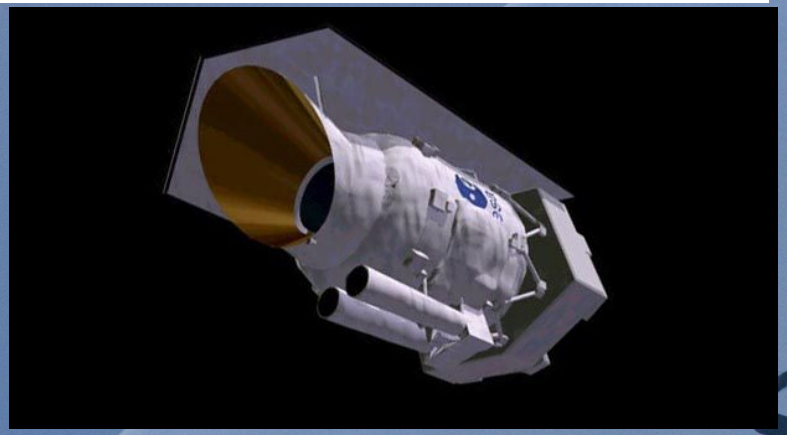

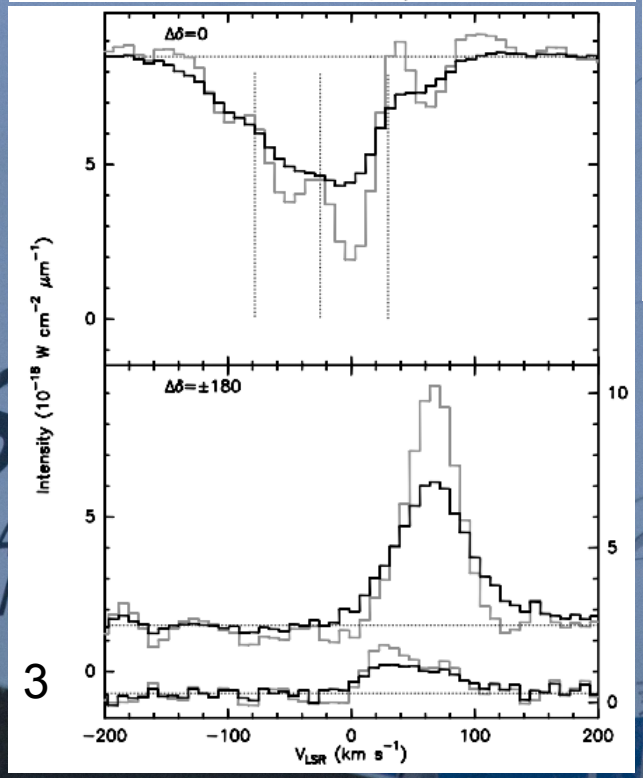

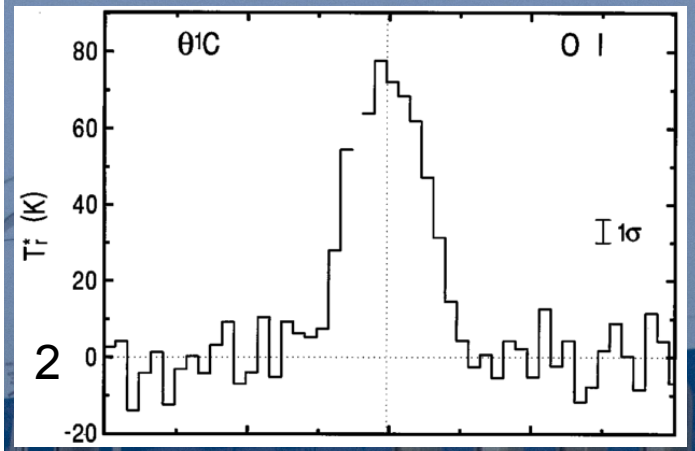

1 – Melnick et al., 1979 (LEARJET)
2 - Boreiko & Betz, 1996 (KAO)
3 - Lis et al. 2001 (ISO-LWS)

Calibration cross-check: PACS HSA data vs. GREAT-H

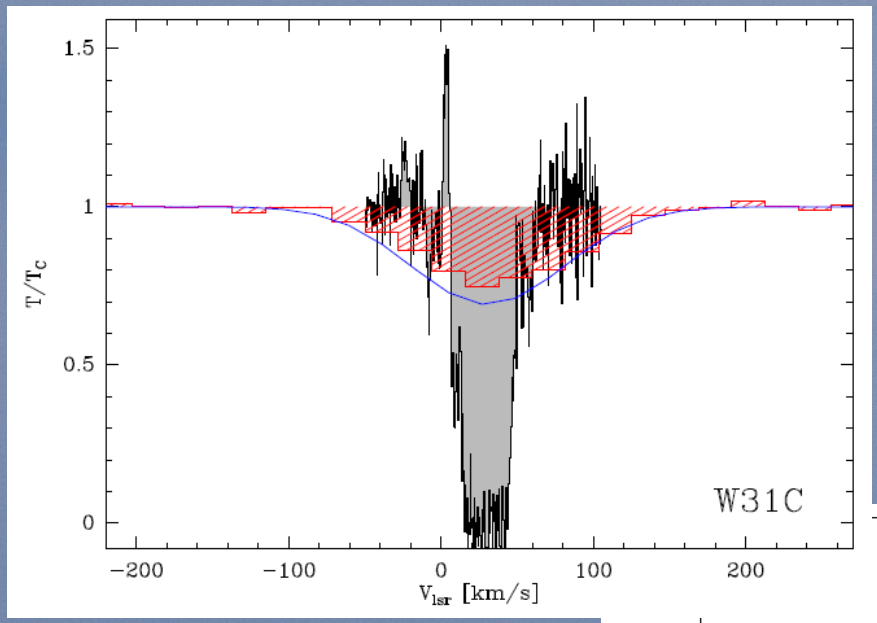

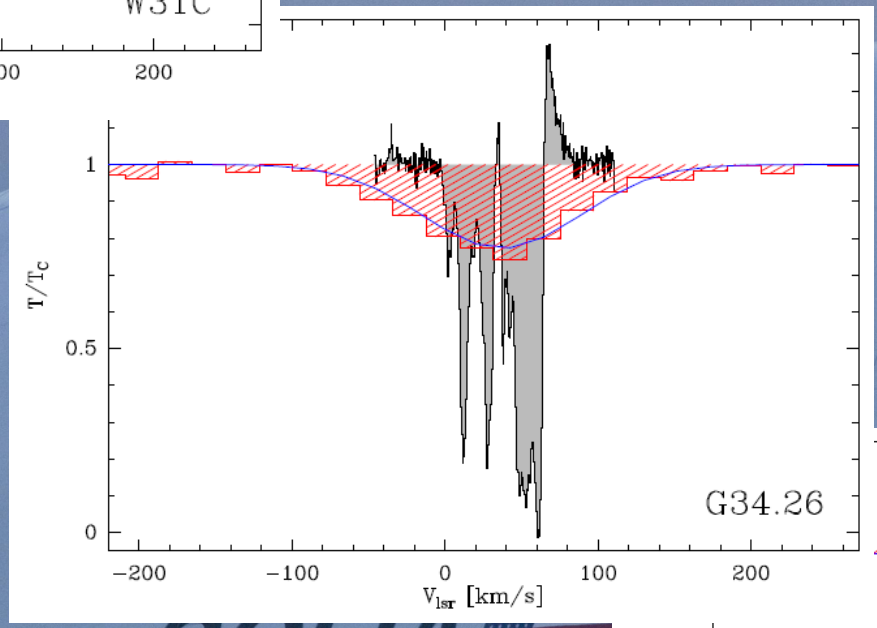

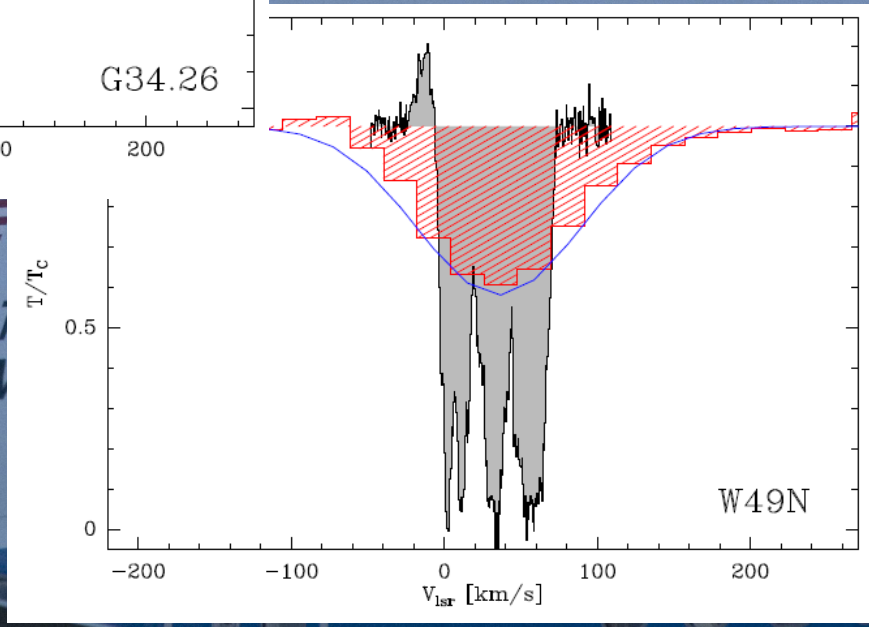

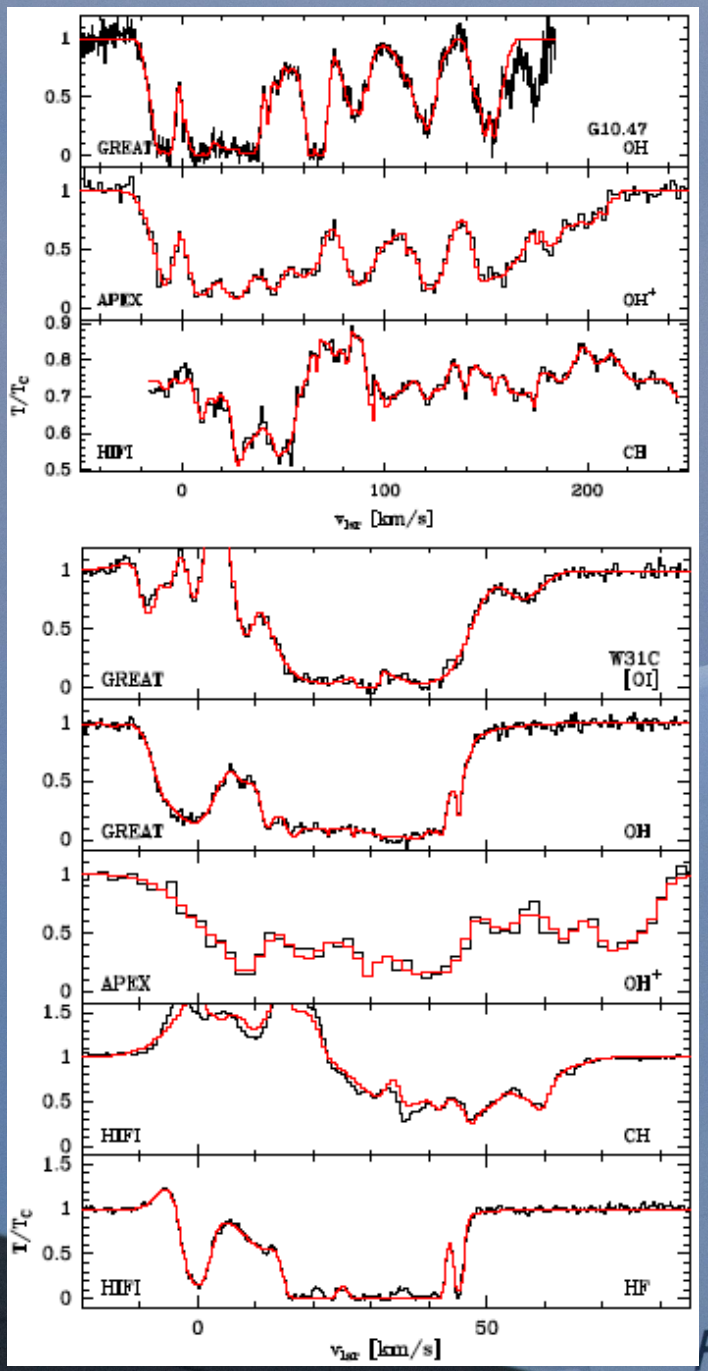
G10.47
GREAT
OH
APEX
OH+
HIFI
CH
HIFI
HF
W31C
[OI]
GREAT
OH
APEX
OH+
HIFI
CH
HIFI
HF
T/Tc
vlsr [km/s]

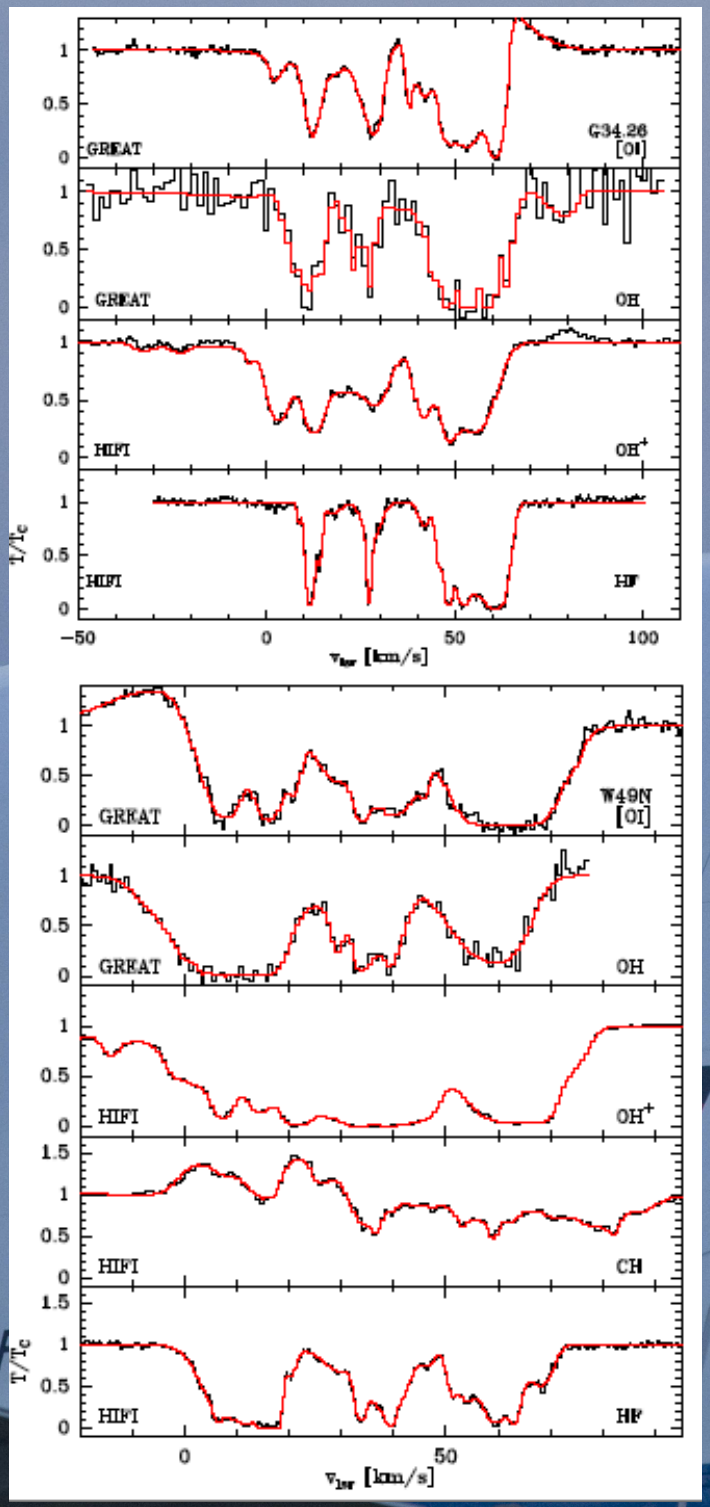
G34.26
[OI]
GREAT
OH
HIFI
OH+
HIFI
HF
W49N
[OI]
GREAT
OH
HIFI
OH+
HIFI
CH
HIFI
HF
T/Tc
vlsr [km/s]

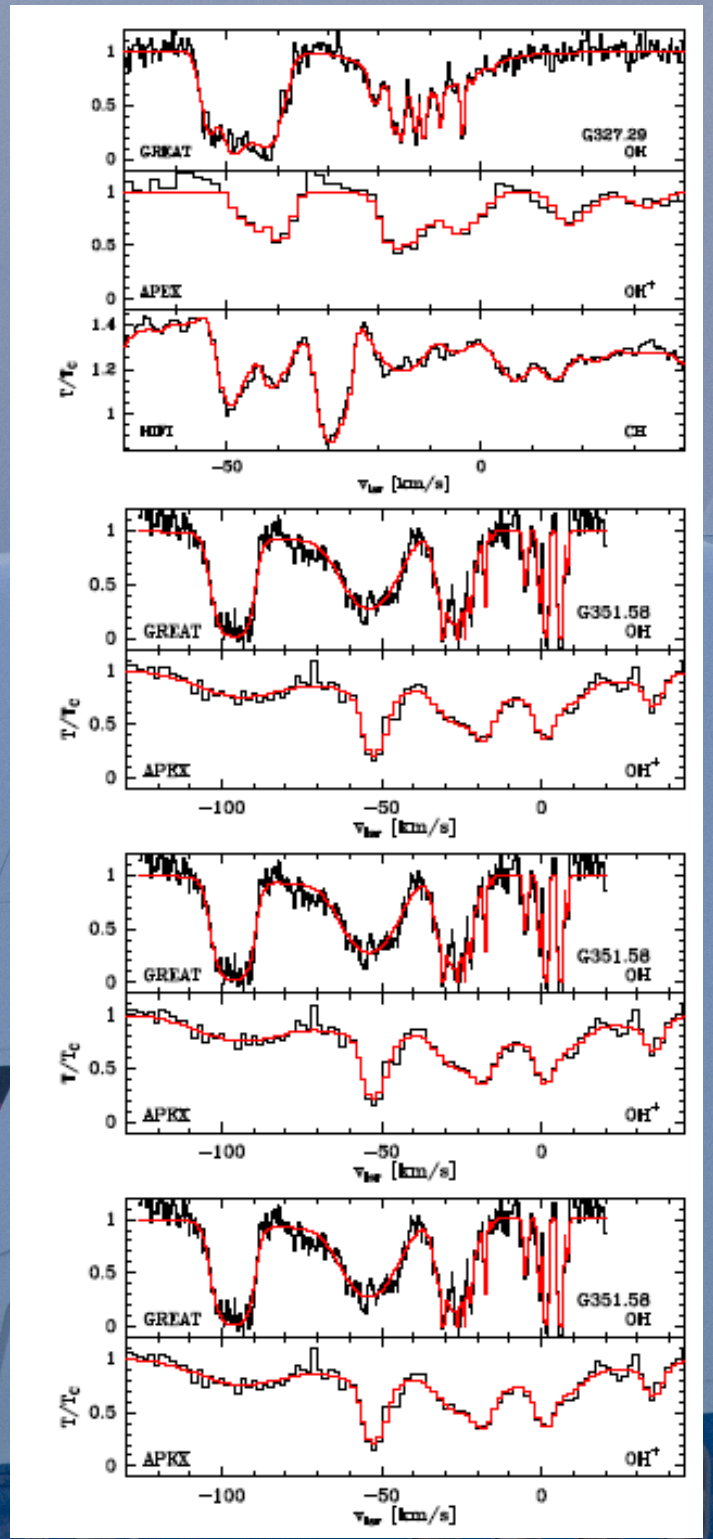
G327.29
GREAT
OH
APEX
OH+
HIFI
CH
G351.58
GREAT
OH
APEX
OH+
G351.58
GREAT
OH
APEX
OH+
G351.58
GREAT
OH
APEX
OH+
T/Tc
vlsr [km/s]

Derived column density profiles

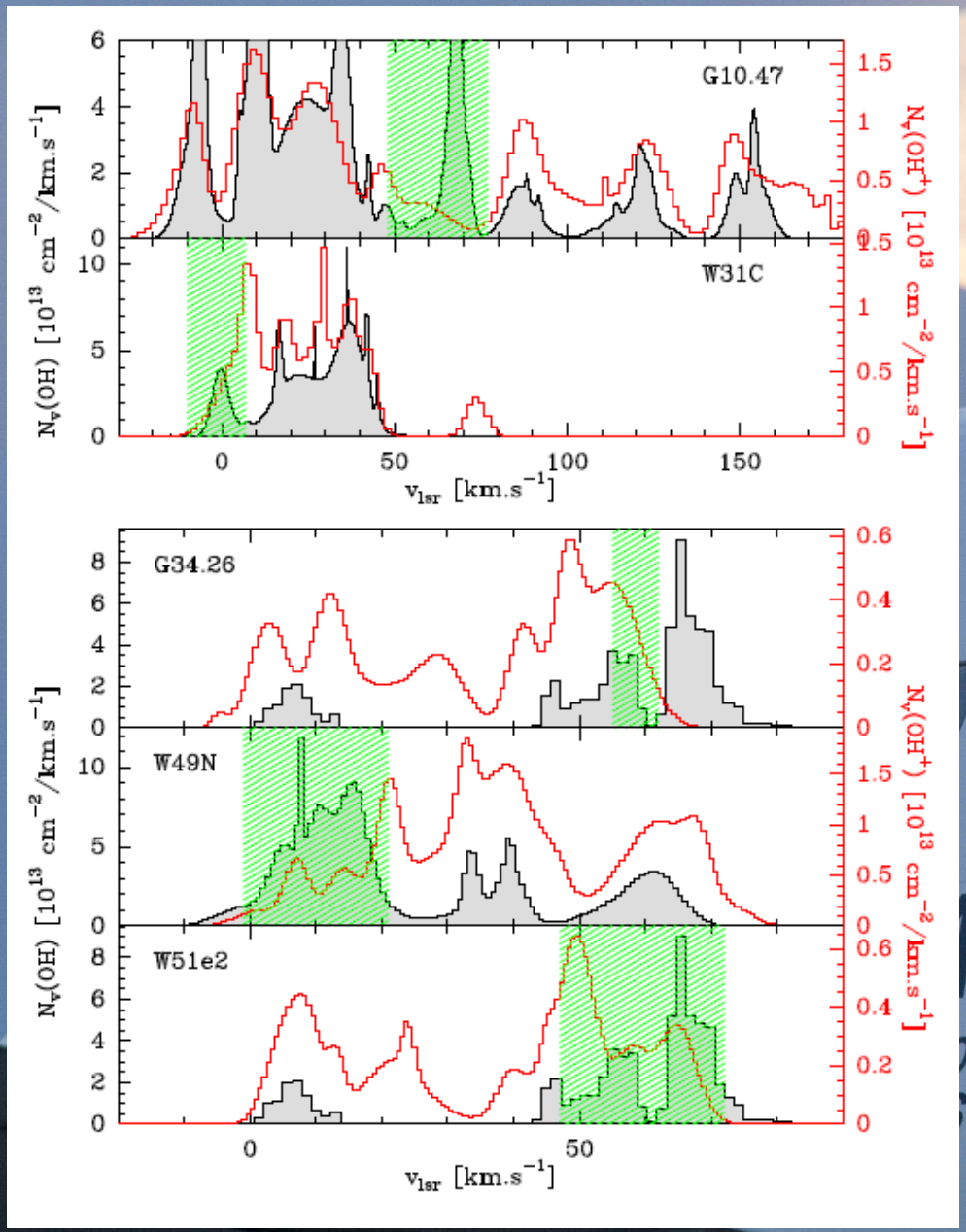

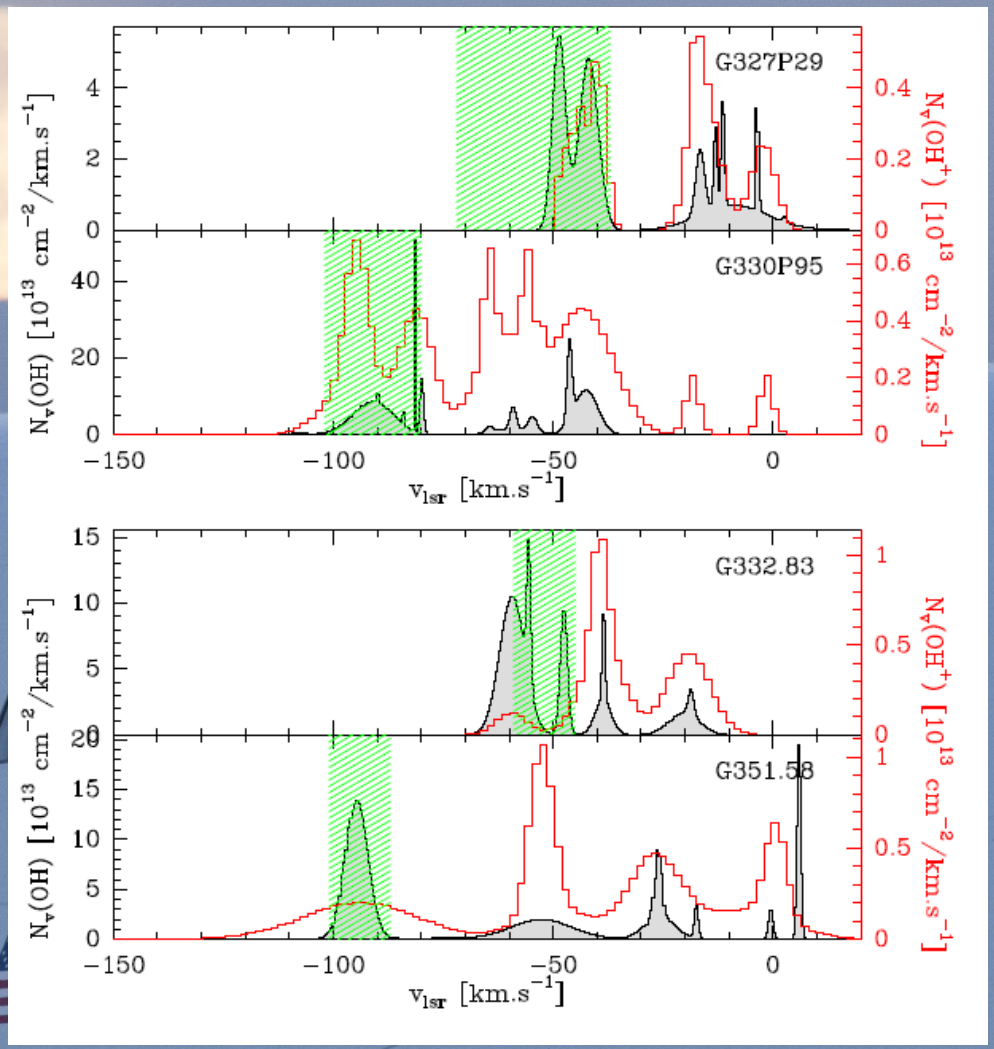

HF and CH as surrogates for H_2

Neufeld & Wolfire 2009, Sonnentrucker et al. 2010, Gerin et al. 2010

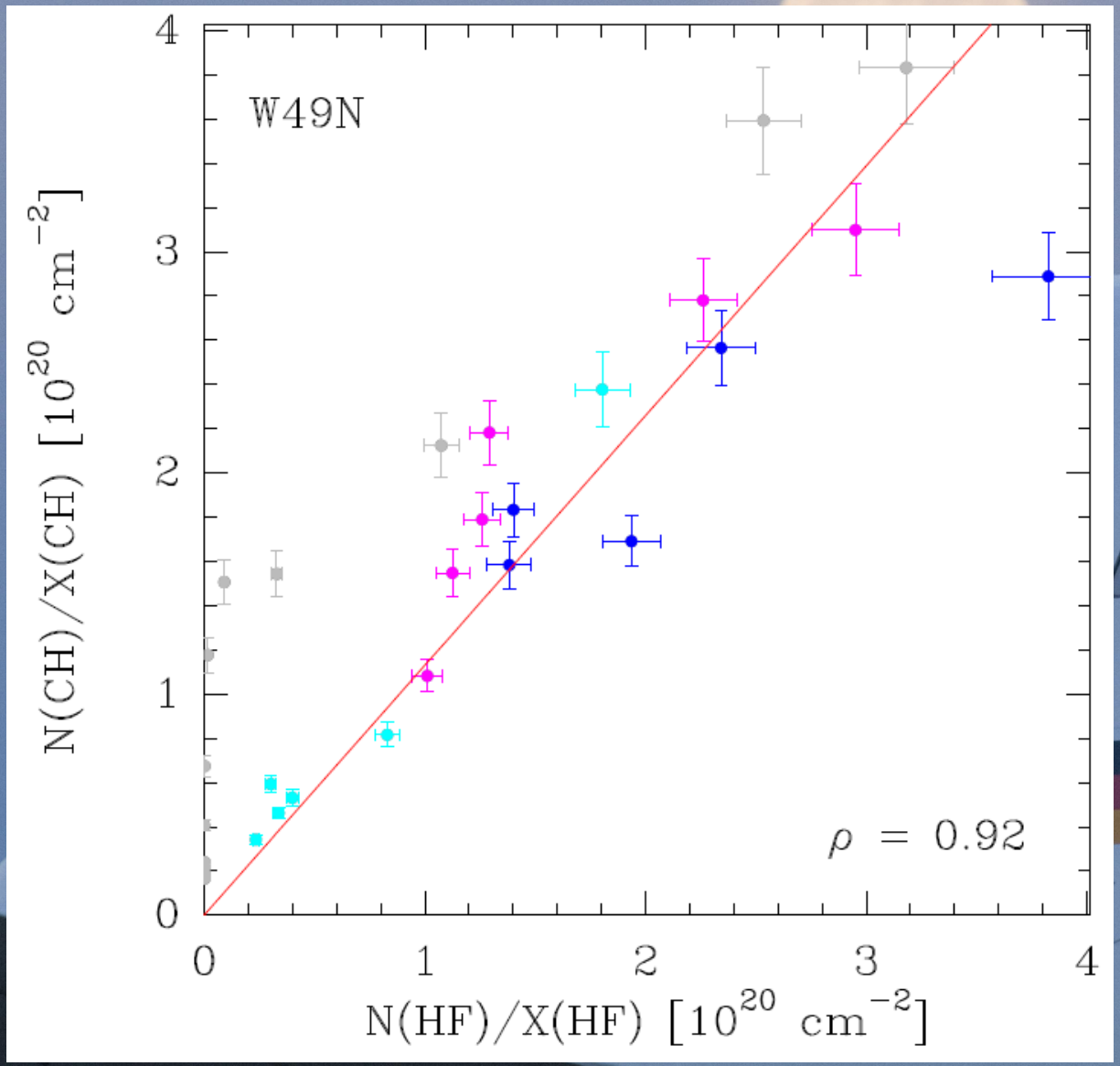

$X(HF) = 3.6 \cdot 10^{-8}$
$X(CH) = 9 \cdot 10^{-8}$

(Godard et al., 2012, A&A 540, A87)

Linear regression suggests ~10% downward correction of X(HF)

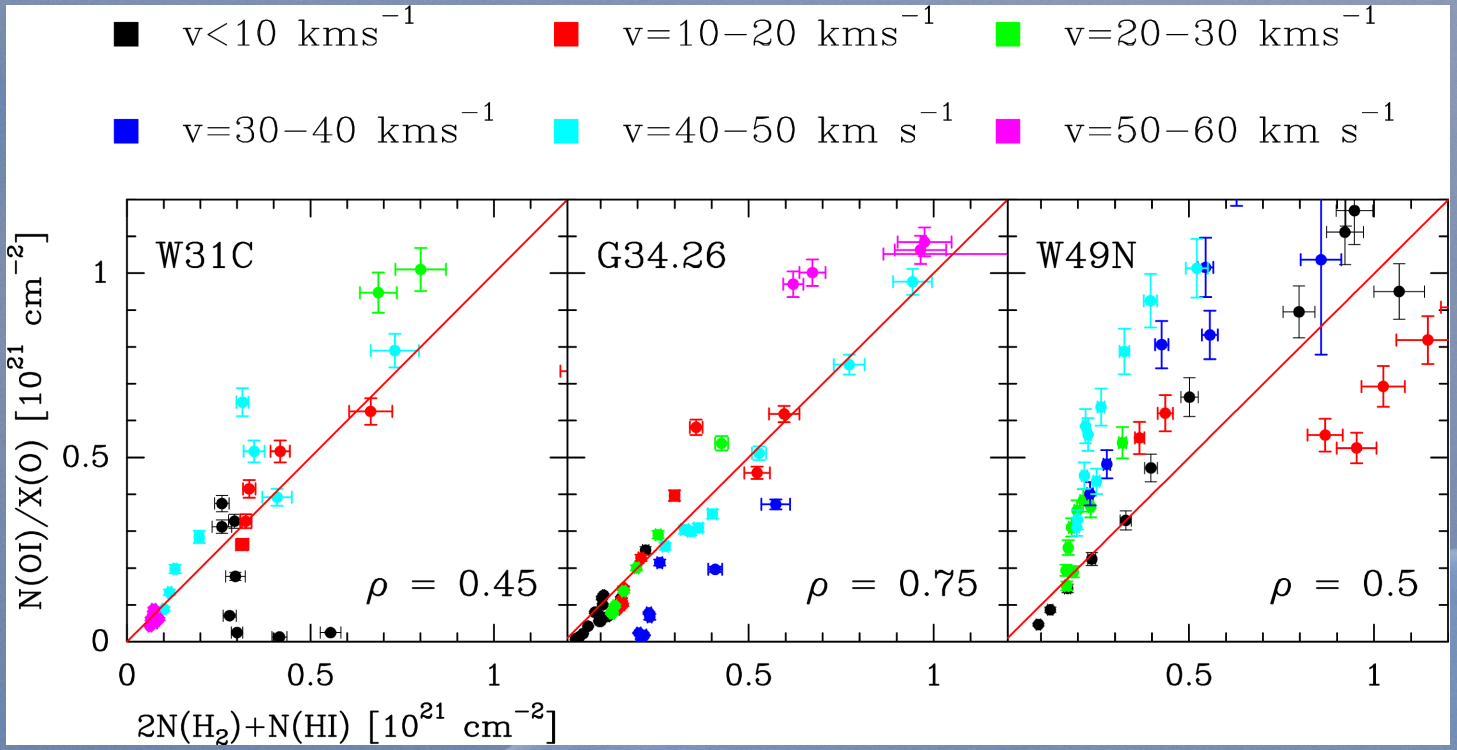

[OI] 63 μm absorption: a proxy for N(HI) +2N(H$_2$) ... up to A$_V$ ~ 1

X(OI) ~ 5 ·10^{-4}

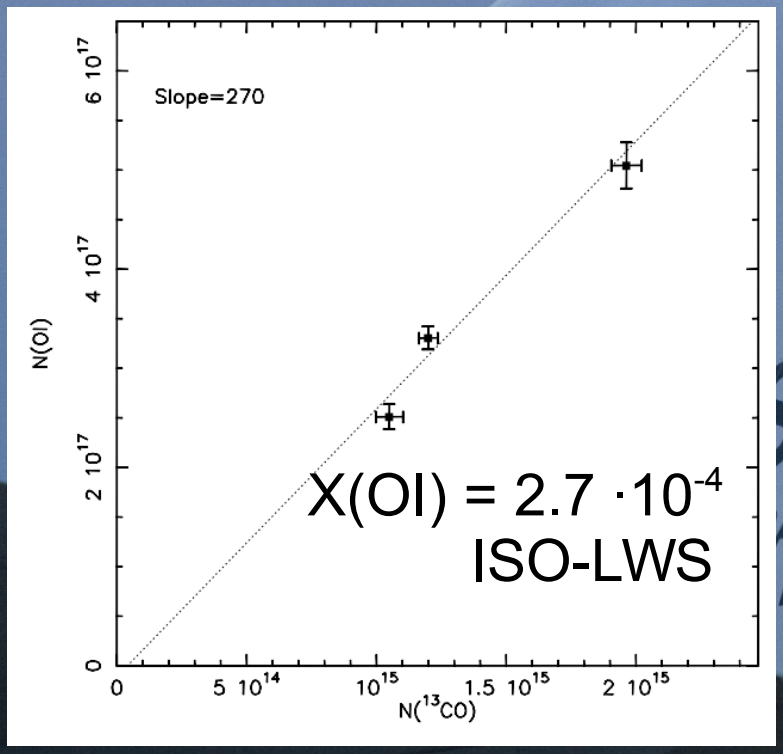

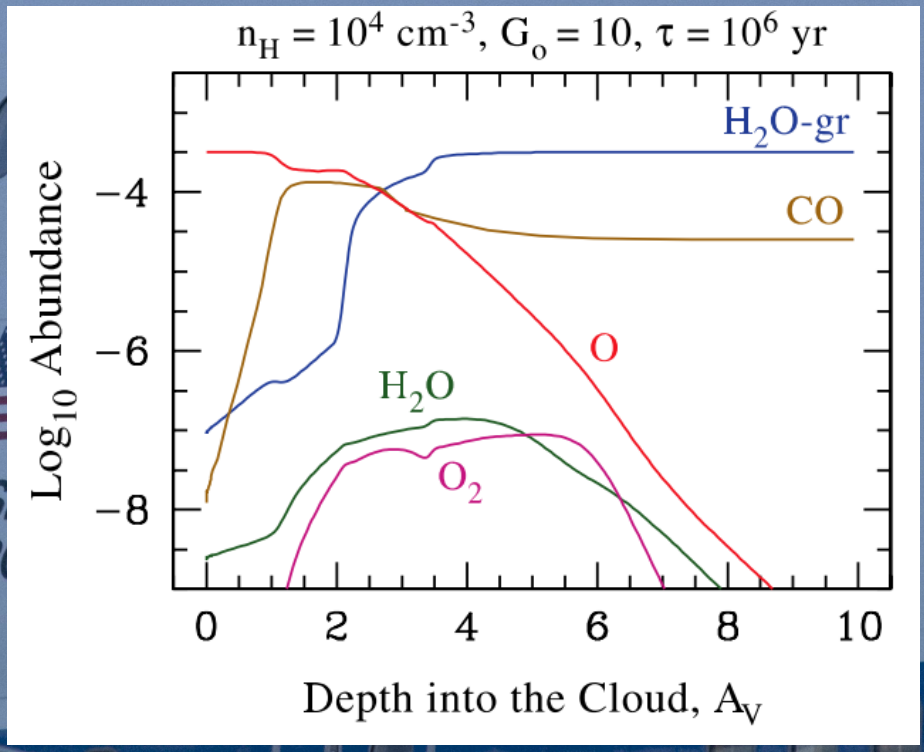

Lis et al., 2001, ApJ 561, 823

Melnick & Bergin, 2005, AdSpRes 36, 1027

OH formation through cold, ion-neutral chemistry

(1) Cosmic ray ionization of H or H_2, followed by $H_2^+(H_2,H)H_3^+(O,H_2)OH^+$ or $H^+(O,H)O^+(H_2,H)OH^+$

(2) Dissociative recombination of OH^+, or : $OH^+(H_2,H)H_2O^+(H_2,H)H_3O^+$

(3) Dissociative recombination of H_3O^+ to OH (~74% to 83%) and H_2O (Jensen et al. 2000, Neau et al. 2000)

(4) Further OH formation by photo-dissociation of H_2O.

(5) … and by endothermic pathway: $O(H_2,H)OH(H_2,H)H_2O$

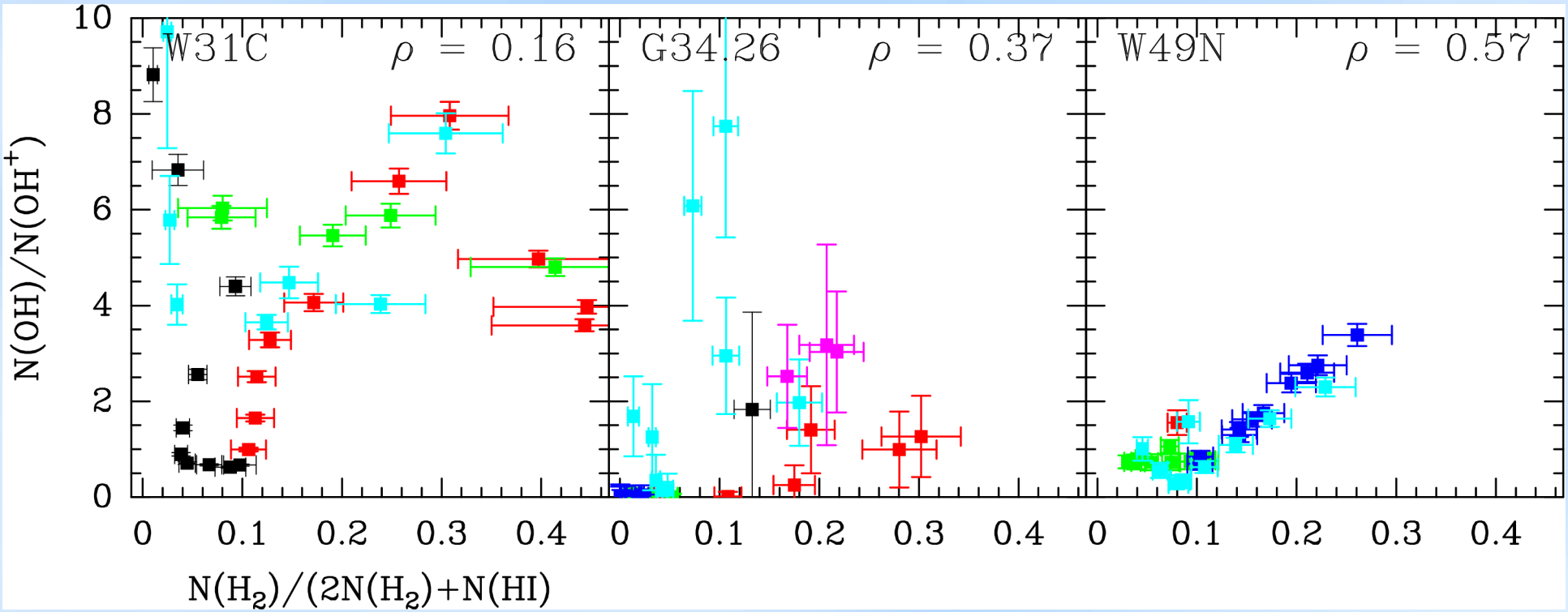

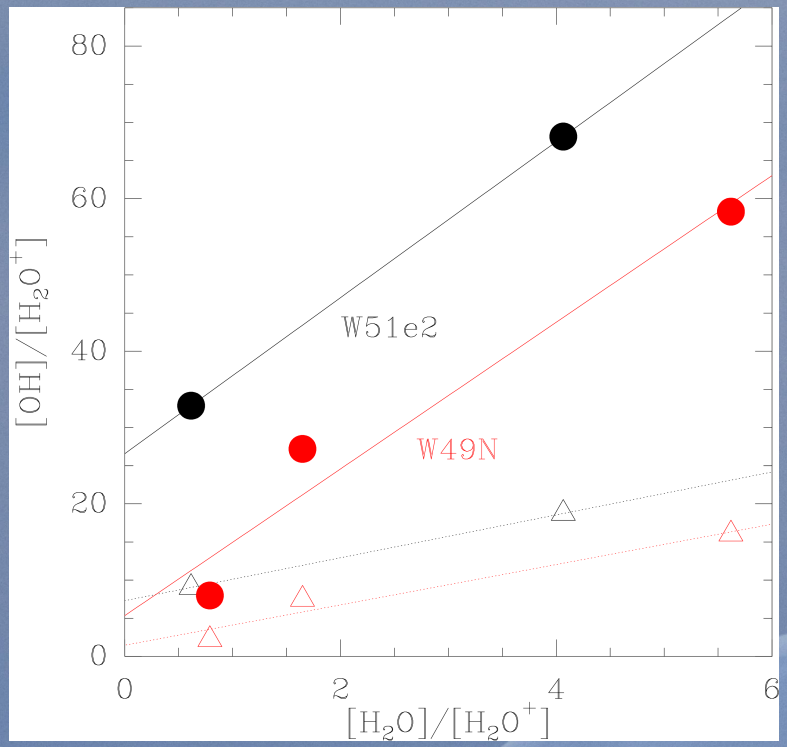

Branching ratio of dissociative recombination of H_3O^+

b = N(OH)/[N(OH)+N(H_2O)]

= **74 %** (W49N), **73%** (W51e2)

for ortho/para = 3:1 →
warm temperature regime,
Albertsson et al. (2014, ApJ 787, 44)

N(H2O+) from Indriolo et al.
(2015, ApJ 800, 40)

Experimental determination:

b = 75%
(Jensen et al., 2000, ApJ 543, 764)
b = 67 – 70%
(Neau, A., et al. 2000, J. Chem. Phys., 113, 1762)

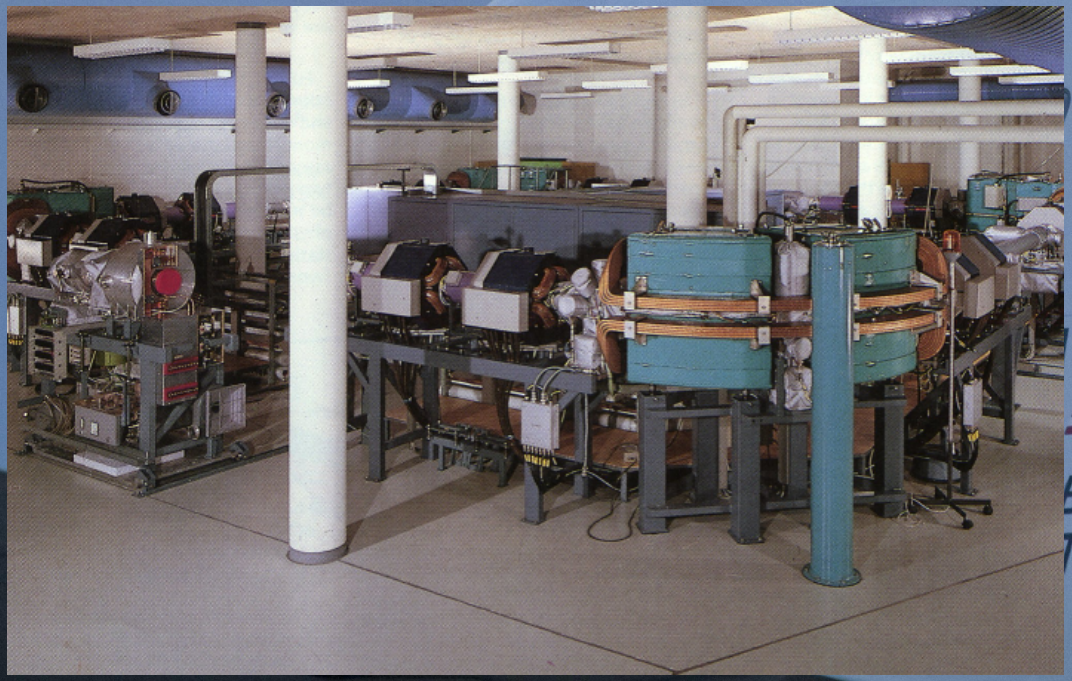

ASTRID Ion storage ring, Aarhus, Denmark

Enhanced water production by dissipation of turbulence ? → $O(H_2,H)OH(H_2,H)H_2O$

Models with time-dependent o/p ratio:
$X(OH) = (0.3 - 1.6) \times 10^{-7}$,
(Albertsson et al. 2014)

Our OH study:
$X(OH) = (0.2 – 8.0) \times 10^{-7}$

Dissipation of turbulence due to ion-neutral friction (Godard et al. 2012, A&A, 540, AA87):

[H2O]/[OH] = 0.16
for $n_H = 100$ cm^{-3}, $A_V = 0.4$

Our study:
[H2O]/[OH] = 0.28 and 0.08
for o/p = 3:1 and 1:10
(warm) (cold)

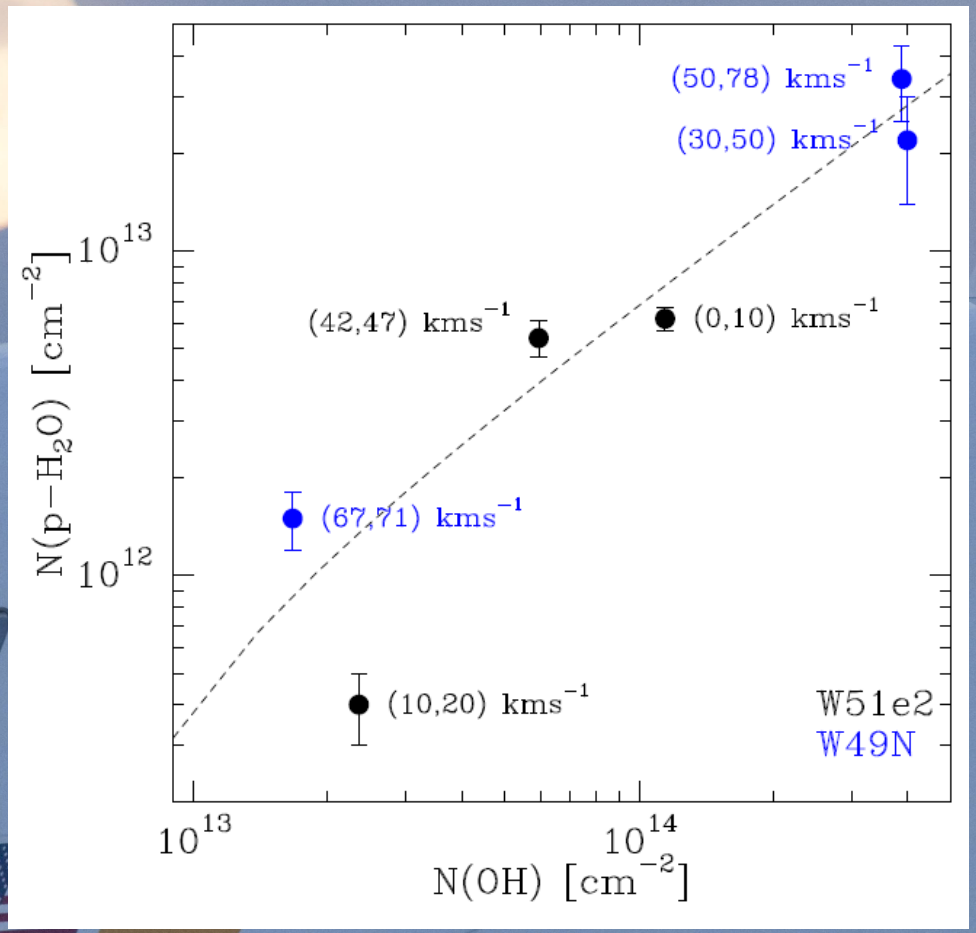

Conclusions – in a nutshell:

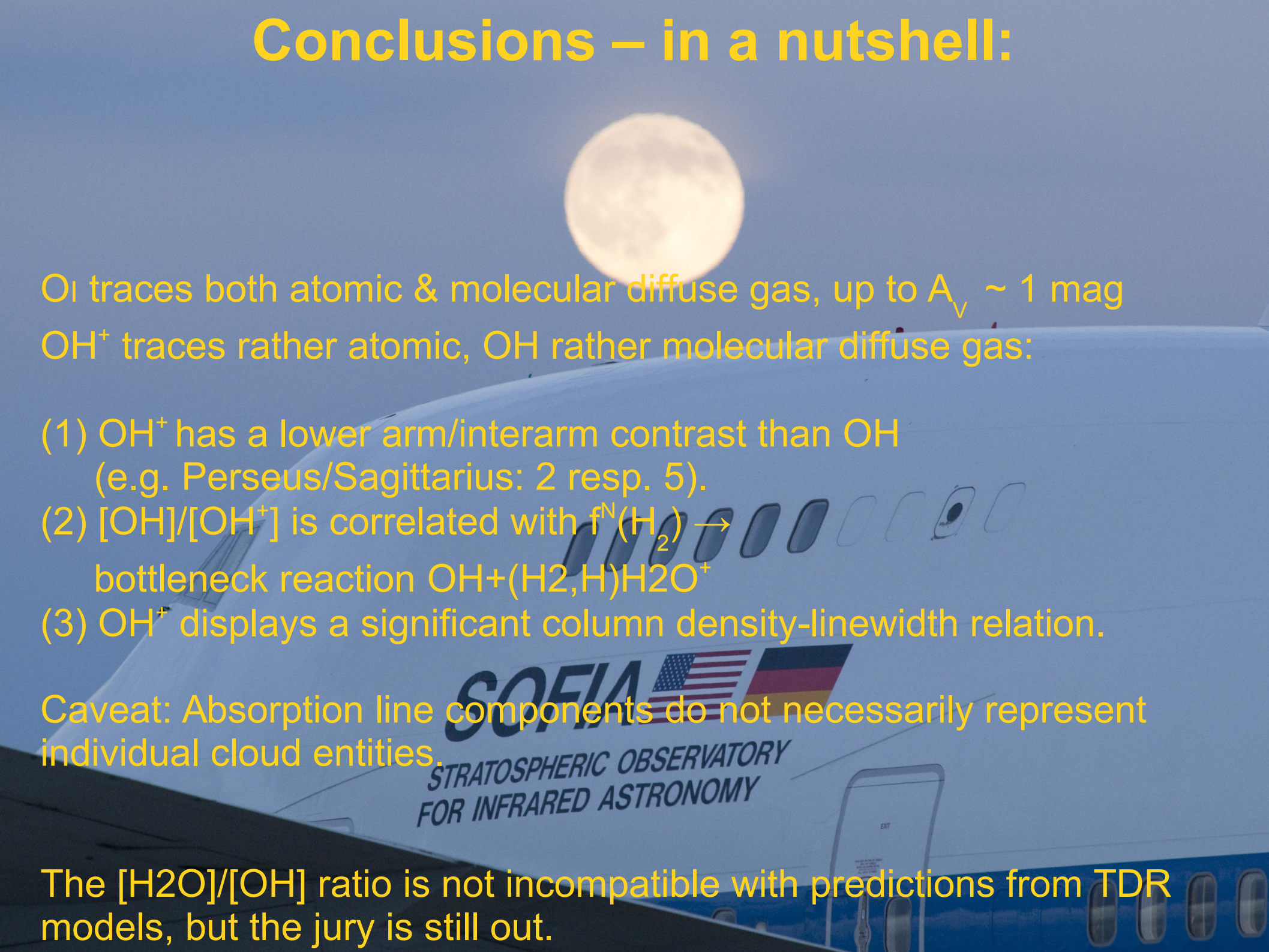

OI traces both atomic & molecular diffuse gas, up to A_V ~ 1 mag

OH^+ traces rather atomic, OH rather molecular diffuse gas:

(1) OH^+ has a lower arm/interarm contrast than OH
(e.g. Perseus/Sagittarius: 2 resp. 5).

(2) [OH]/[OH^+] is correlated with $f^N(H_2) \rightarrow$
bottleneck reaction OH+(H2,H)H2O$^+$

(3) OH^+ displays a significant column density-linewidth relation.

Caveat: Absorption line components do not necessarily represent individual cloud entities.

The [H2O]/[OH] ratio is not incompatible with predictions from TDR models, but the jury is still out.

We GREATfully acknowledge the support by the observatory staff.

Thank you.